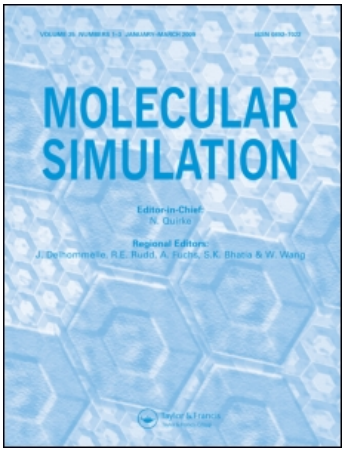

Molecular Simulation
Publication details, including instructions for authors and subscription information:
http://www.informaworld.com/smpp/title~content=t713644482

Computer Modelling of Phosphate Biominerals: Parameterisation for Perfect Lattice Calculations

M. G. Taylor[a]; K. Simkiss[a]; M. G. B. Drew[b]; P. C. H. Mitchell[b]; M. Leslie[c]
[a] Department of Pure and Applied Zoology, University of Reading, Reading, U.K. [b] Department of Chemistry, University of Reading, Reading, U.K. [c] SERC Daresbury Laboratory, Warrington, U.K.

To cite this Article Taylor, M. G. , Simkiss, K. , Drew, M. G. B. , Mitchell, P. C. H. and Leslie, M.(1992) 'Computer Modelling of Phosphate Biominerals: Parameterisation for Perfect Lattice Calculations', Molecular Simulation, 9: 2, 129 — 141
To link to this Article: DOI: 10.1080/08927029208050606
URL: http://dx.doi.org/10.1080/08927029208050606

Molecular Simulation, 1992, Vol. 9, pp. 129–141
Reprints available directly from the publisher
Photocopying permitted by license only

COMPUTER MODELLING OF PHOSPHATE BIOMINERALS: PARAMETERISATION FOR PERFECT LATTICE CALCULATIONS

M.G. TAYLOR and K. SIMKISS

Department of Pure and Applied Zoology, University of Reading, Whiteknights, Reading, RG6 2AJ, U.K.

M.G.B. DREW and P.C.H. MITCHELL

Department of Chemistry, University of Reading, Whiteknights, Reading, RG6 2AJ, U.K.

and

M. LESLIE

SERC Daresbury Laboratory, Warrington, WA4 4AD, U.K.

(*Received November 1991, accepted December 1991*)

We are extending the use of the method of static simulation of ionic lattices to modelling phosphates and condensed phosphates, the mineral components of many biominerals whose structure, crystallinity and reactivity can be influenced by substitutions and other defects. Parameters for the interatomic potentials of some phosphates and pyrophosphates have been determined and we present our results for the modelling of α-magnesium pyrophosphate, a representative compound of moderate complexity. The approach has been to treat the compound as an ionic solid with Mg^{2+} as the cation and $P_2O_7^{4-}$ as a predominately covalent anion which is, however, ionically bound to the metal. Good agreement was found between the calculated and experimental structures for this ionic model using formal or residual charges, a Born–Mayer term for non-bonded repulsive interactions, whose parameters were calculated using the electron gas technique, a van der Waals dispersion term and three body terms to account for the directionality of bonding in the phosphate groups in the tetrahedra.

KEY WORDS: Biominerals, static lattice simulations, interatomic potentials, electron gas

1 INTRODUCTION

Phosphate biominerals are a class of materials that are of growing importance in both fundamental and applied studies. Hydroxyapatite ($Ca_5(PO_4)_3OH$) occurs with varying amounts of carbonate and fluoride in the mineral phase of bones and teeth. Pyrophosphates (diphosphates, $[P_2O_7]^{4-}$) may occur in trace amounts as precursors of bones but they can also occur in joints as calcium pyrophosphate dihydrate crystals giving rise to pseudogout. In the amorphous form magnesium and calcium pyrophospates are also present in some urinary calculi and in granules in blood platelets [1, 2]. Thus, in vertebrates, these minerals may occur as ortho- or pyrophospate in either crystalline or amorphous forms. These same materials are also widespread among a wide range of invertebrates often as intracellular granules enclosed within a membrane delimited space. They are typically calcium and magnesium cations with ortho- or

pyrophospate anions [3] but in many organisms accumulate other cations such as manganese and zinc [4]. In all cases, however, it is clear that the degree of crystallisation of these materials and their surface reactivities are strongly influenced by their substituent ions and by defects in their lattice. These features determine most of the properties of these important biominerals but the distribution of the cations is unknown and, where mixed deposits are involved, could give rise to regions of solid solutions or biphasic materials. To investigate the cation distribution and to determine the effects of cation substitution defects on the perfect lattice parameters and the energetics of these substitutions we are using computer modelling.

As a first step we have calculated parameters for interatomic potentials in a number of pyrophosphate and orthophosphate compounds for which we have structural information in order to test the potentials. Here we present our methods and the results for anhydrous α-magnesium pyrophosphate as a representative compound of moderate complexity.

2 STRUCTURES

The structures of pyrophosphates have been reviewed [5]. Pyrophosphate is a dimer of two phosphate tetrahedra sharing a corner oxygen. There are two structural types, dichromate (e.g., $K_2Cr_2O_7$) and thortveitite ($Sc_2Si_2O_7$). These are distingiushed by the conformation of the phosphate (PO_3) groups Figure 1(a), (b). In the dichromate structure type they are essentially eclipsed and the POP bridging angle is less than 140°. In some metal pyrophosphates the bridging oxygen is in the first coordination sphere, (e.g. β-$Ca_2P_2O_7$, [6]). The conformation may also be stabilised by the bonding of the cation to both halves of the dimer (e.g. α-$Ca_2P_2O_7$, [7]). In the thortveitite structure the PO_3 groups are staggered and there is no cation bonding to the bridging oxygen. The bridging angle is greater than 140°. While linear POP angles of 180° in, for example, the β- forms of magnesium, manganese and zinc pyrophospate, have been reported in crystal structures it seems likely that this is a mean value reflecting disorder and a crystallographic centre of symmetry [8]. By contrast in some pyrosilicate structures the linear bridge has been unambiguously established [5].

A feature of both structure types of $[P_2O_7]^{4-}$, is the range of bond orders and hence bond distances of the phosphorus oxygen bonds in the distorted tetrahedral phosphate units and consequently the cation and oxygen distances [9]. A molecular orbital approach for phosphorus–oxygen bonding suggests sp^3 hybridisation and the formation of four phosphorus oxygen σ bonds in a tetrahedral geometry. Further $d\pi$–$p\pi$ bonding arises from combinations of oxygen $2p\pi$ orbitals and phosphorus $3d$ orbitals, $3d_{x^2-y^2}$ and $3d_{z^2}$ [10]. Generally the P–O bonds lengths in phosphates average 1.54 Å and thus are shorter than expected for a single bond 1.71 Å. This is also true of the P–O_B bond distances which range from 1.56 to 1.63 Å [11]. Often at least one of the bonds shows considerable double bond character [12, 13]. The property determines the ability to form extended network structures in glasses as there is a limited ability to use all the oxygens in linking units and contrasts with the Si–O tetrahedron in which each Si–O bond is more equivalent. The cations will therefore often stabilise the network in phosphate glasses but also exhibit a range of bond distances and coordination numbers. The consequence is that some of these compounds do not crystallise readily at ambient temperatures and substitutions can lead to amorphous structures.

To simulate such compounds presents many challenges. Many of the cations of interest such as magnesium, calcium and manganese interact in an essentially ionic way, zinc will be expected to exhibit more covalency. Aluminium phosphate bonding will be largely covalent as will all the binding in the anionic part of the pyrophosphate units.

Magnesium pyrophosphate exists in a low temperature α-form and a high temperature β-form. Both structures [8, 14] are related to the thortveitite structure which exhibits a bridging P–O_B–P (O_B indicates bridging oxygen) angle greater than 140° ($\alpha = 144°$, $\beta = 180°$), a staggered conformation of the PO_3 groups and the cations do not approach the bridging oxygen close enough to form a bond. In the α-form the two independent magnesium cations are five and six coordinate whereas in β-form both cations are six coordinate in a distorted octahedral environment. In the α-form, Figure 2, the Mg–O bond distances range from 1.98 to 2.142 Å and in the β-form from 2.02 to 2.15 Å.

3 THEORETICAL METHODS

3.1 Introduction

Classical energy minimisation techniques [15], method of steepest descent and Newton–Raphson, have been used widely in static lattice simulations of perfect and defect structures. Much of the early work was concerned with metal oxides; more recently this has been extended to modelling silica and silicates and zeolites [16, 17]. The lattice energy of the compound is computed as the sum of the long range Coulombic interactions summed by the Ewald method, [18], the short range non-bonded potentials which decay quickly and force field terms which may include two, three and four body interactions.

$$E(\text{eV}) = E_{\text{COULOMBIC}} + E_{\text{SHORTRANGE}} + E_{\text{THREEBODY}} \quad (1)$$

The lattice energy is minimised as a function of structural parameters such as unit cell dimensions, atomic coordinates, bond lengths and bond angles. At the minimum the derivatives of the energy with respect to the geometric factors will be zero.

To calculate the relaxed perfect lattice of a α-$Mg_2P_2O_7$ and so test the parameters for the interatomic potentials and force constants, the THBREL and PHONON programs available under the SERC CCP5 scheme have been used [19, 20]. The model is ionic but the inclusion of three body terms has enabled the successful application of the programs in the modelling of silicates which present similar problems to the phosphates. The validity of using the ionic model for such compounds was discussed and reviewed by Catlow and Stoneham [21]. Our approach has been to treat α-magnesium pyrophosphate as an ionic solid with Mg^{2+} as the cation and $P_2O_7^{4-}$ as a predominately covalent anion which is, however, ionically bound to the metal. Oxygen forms bonds with magnesium but is also part of the pyrophosphate unit so is clearly not equivalent to the oxygen of magnesium oxide which carries a 2^- charge and therefore we have developed new parameters.

3.2 Interatomic Potentials

Central to any simulations are the interatomic potentials for the compounds of interest.

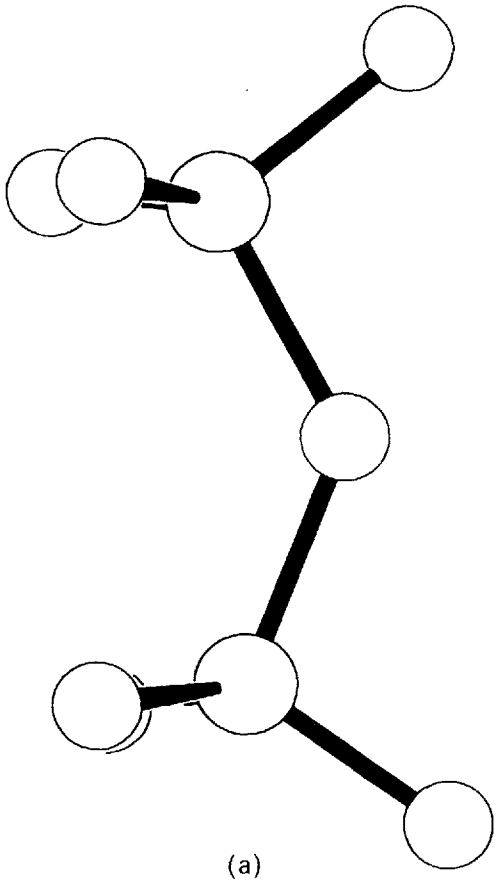

Figure 1 Conformations of the $P_2O_7^{4-}$ anion. (a) The $P_2O_7^{4-}$ anion in the β-$Ca_2P_2O_7$ structure. The PO_3 groups are eclipsed, indicative of the dichromate structural type. (b) The $P_2O_7^{4-}$ anion in the α-$Mg_2P_2O_7$ structure. The PO_3 groups are staggered, indicative of the thortveitite structural type.

The energy of interaction between two ions i and j with charges q_i and q_j is given by the following Equation (2).

$$V_{ij}(r_{ij}) = q_iq_j/r_{ij} + A_{ij}\exp(-r_{ij}/\rho_{ij}) - (\chi_D(r_{ij})C_6(ij))/r_{ij}^6. \quad (2)$$

The first term represents the electrostatic Coulombic interactions between each pair of ions. The second term is the non-bonded repulsive terms arising from the overlap of the electron clouds of the approaching ions and is the analytic form of the Born–Mayer equation and lastly the dispersion term is due to the van der Waals attractive forces derived by Slater and Kirkwood [22]. Here χ_D is a damping factor which is also a function of r [23]. In addition terms for the pyrophosphate anion incorporating the two and three body vibrations have been included. Three bending terms account for the strong directional bonding in the anion.

$$V_{3-\text{body}} = 1/2k_B(\theta - \theta_0)^2 \quad (3)$$

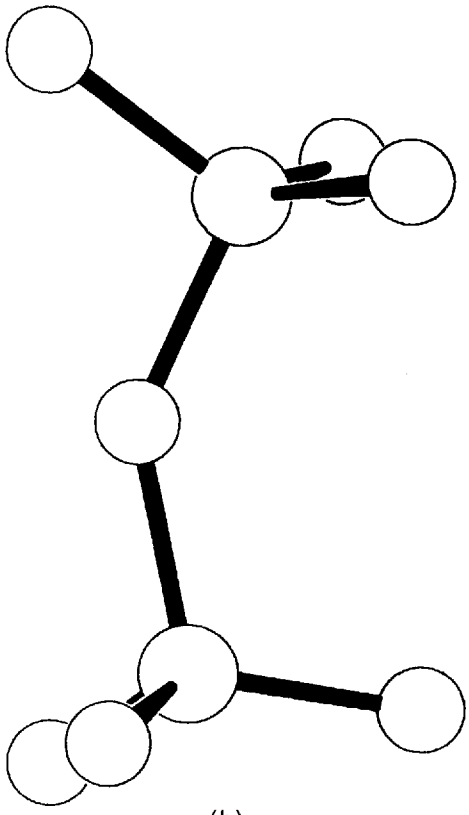

(b)

Figure 1 Continued.

where k_B is the bond bending force constant and θ_0 is the equilibrium bond angle. Harmonic spring constants for the two body terms were derived empirically using force constants calculated from the vibrational spectrum of α-magnesium pyrophosphate [24, 25]. Force constants for the three body bending modes were also derived empirically by taking account of the regions of the infrared spectrum where these vibrations occur.

Parameters for the short range potentials can be determined by three methods. In the first method, parameters are obtained by empirical fitting to the crystal structure and known tensor properties of the system such as elastic and dielectric constants. This technique has been used successfully in modelling metal oxides and many silicate structures. Since the amount of experimental data for our system is limited we have been reluctant to use this method. The second technique uses *ab initio* calculations as proposed by Pyper [23]. However, at present such methods are not feasible for the complexity of pyrophosphate structures and would require too much computer resources.

The third method uses the electron gas technique encoded by Harding and Harker [26] and based on the work of Wedephol [27] and Gordon and Kim [28]. This method

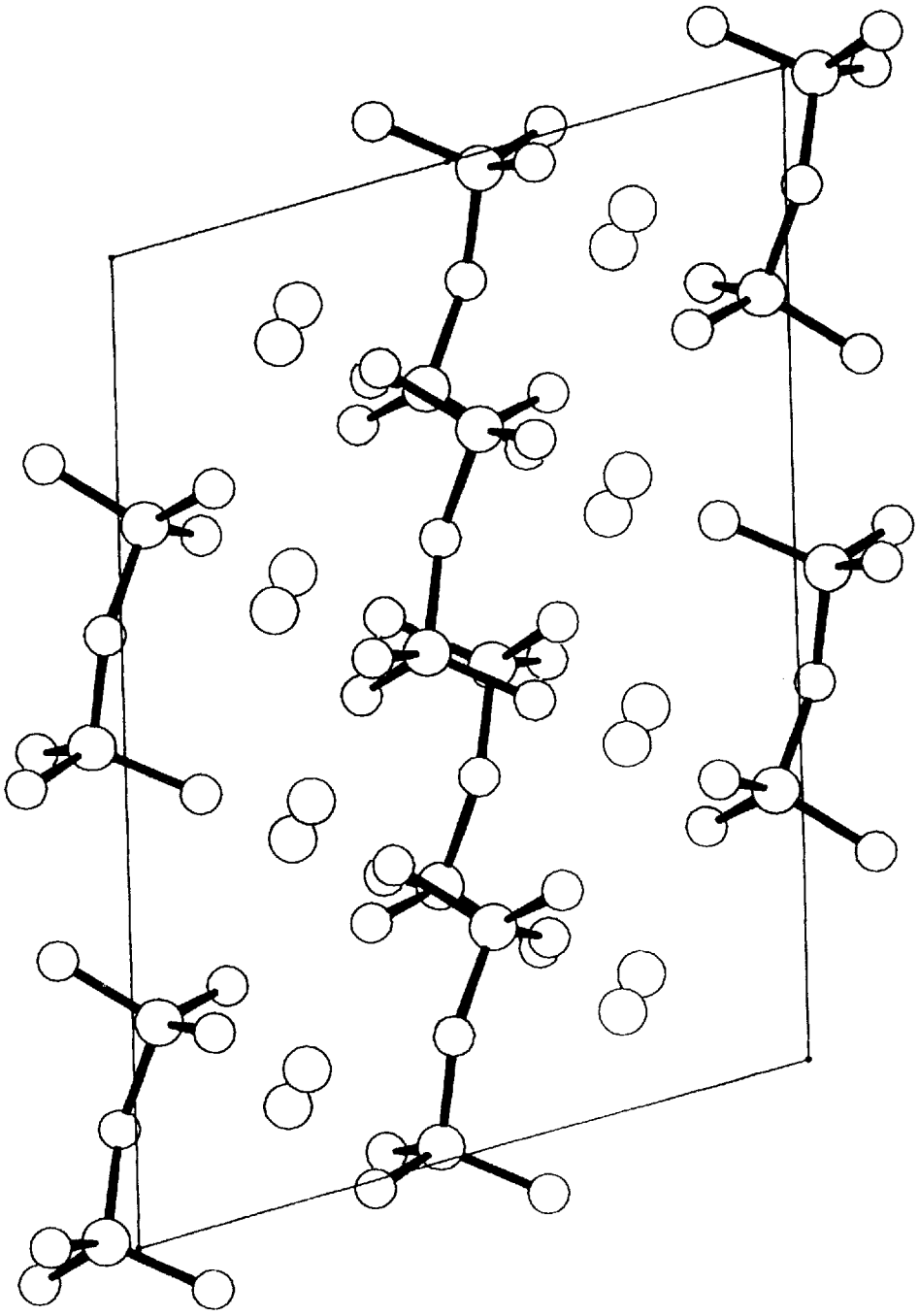

Figure 2 The unit cell of a α-$Mg_2P_2O_7$ in the b projection showing layers of pyrophosphate units and Mg^{2+} cations. For clarity the Mg–O bonds are not indicated.

Table 1 Charge models of α-Magnesium Pyrophospate.

Charges	*Model I* *Full ionic*	*Model II* *Formal*	*Model III* *Fractional*
Magnesium	+2	+2	+2
Phosphorus	+5	+1	+0.750
Oxygen-B	−2	0	−0.250
Oxygen-T	−2	−1	−0.875

provides an independent theoretical basis for parameterisation and as we shall show works well for pyrophosphate. The model calculates the forces between closed shell atoms or ions. It is assumed that the charge density of the ion pair is the sum of the separate charge densities. The resulting interatomic potentials may be fitted to an analytic form such as the Born–Mayer equation. It should be possible to use these potentials in both static and dynamic simulations [26].

$$E_{\text{interaction}} = E_{\text{electrostat}} + E_{\text{kin}} + \mathrm{E}_{\text{exch}} + E_{\text{corr}} \tag{4}$$

The energy of interaction takes account of electrostatic (electrostat) energy, kinetic (kin) energy, exchange (exch) energy and correlation (corr) energy, each of which can be expressed in terms of the charge density functions. The interaction energies for the atoms in the pyrophosphate unit were calculated from expansions of the Slater functions modified to account for the Madelung potential experienced in the crystal. They were averaged over configurations to give spherically symmetrical ions. As magnesium is located in a spacious site the Clementi free ion function was used. The final term, involving the van der Waals many electron dispersion coefficients was calculated using the formula derived by Slater and Kirkwood [22]. for the interaction between species i and j

$$\mathrm{C}_6(ij) = 3/2\alpha_i\alpha_j/[(\alpha_i/\mathrm{P}_i)^{1/2} + (\alpha_j/\mathrm{P}_j)^{1/2}] \tag{5}$$

which for two equivalent species becomes

$$\mathrm{C}_6(ii) = 3/4\alpha_i^{3/2}\mathrm{P}_i^{1/2} \tag{6}$$

where α_i is the static polarizability of species i and P_i the effective number of electrons contributing to the polarizability. A damping parameter $\chi_{Dij}(r)$ has been included to reduce the dispersion energies when the wavefunction overlap is not negligible [23].

Whilst recognising that polarisabilities in the pyrophosphate anion are likely to be important we have not at this stage used the shell model whereby the valence charge of a massless shell and the mass containing core charge is coupled by a harmonic spring hence allowing the polarisation effects to occur by the displacement of the shell relative to the core [29].

4. RESULTS AND DISCUSSION

The first step for our calculations of the short range repulsive interactions was to set up charge models for the pyrophosphate unit in order to determine the Madelung potentials for the calculation of the atomic wave functions. These are given in Table 1. Although we are treating our compounds as ionic the pyrophosphate unit has a large percentage of covalent character, approximately 61% based on Pauling's electronegativities. It was decided to keep an integral charge on the cation of 2^+ to facilitate

Table 2 Calculated parameters for the Buckingham† interatomic potentials for Models I and II*, for simulating the perfect lattice of α-magnesium pyrophosphate

Species	*Parameter*	*Model I Mean value*	±	*Model II Mean value*	±
$Mg-O_T$	A/eV	6059.94	608.36	2551.55	225.71
	ρ/Å	0.21326		0.24332	
	C_6/eVÅ^6			6.0	
O_T-O_T	A/eV	5905.13	186.54	1394.53	148.77
	ρ/Å	0.25599		0.29782	
	C_6/eVÅ			120.00	
O_T-O_B	A/eV	6700.61	171.81	1081.82	78.83
	ρ/Å	0.25144		0.30357	
	C_6/eVÅ^6			80.00	
O_B-O_B	A/eV	–		764.00	
	ρ/Å	–		0.32000	
	C_6/eVÅ^6			53.00	
$P-O_T$	A/eV	6198.06	407.17	270.72	5.96
	ρ/Å	0.21095		0.42876	
	C_6/eVÅ^6			2.00	
$P-O_B$	A/eV	7369.53	20.25	388.48	3.75
	ρ/Å	0.20371		0.39978	
	C_6/eVÅ^6			2.00	
P–P	A/eV	2381.84		1030.43	
	ρ/Å	0.24210		0.35662	
	C_6/eVÅ	–		–	

† $V_{ij}(r) = A \exp(-r_{ij}/\rho) - C_6(ij)$. See text for details of the calculations.
*See Table 1.

future work on cation substitutions. Nevertheless Model I has been constructed with full ionic charges. Although intuitively a 5^+ charge on phosphorus is unrealistic considering the ionisation potentials silicon with a 4^+ charge has worked well in modelling silica and silicates. Each oxygen then carries a charge of 2^- [30]. Our second model is based on Langmuir's formal charges as described by Pauling [12] whereby each atomic pair contributes an electron to a pair bond thus leaving two terminal oxygens with a single negative charge and the bridging oxygen neutral. The third terminal phosphorus–oxygen bond in this scheme also carries a single negative charge as both of the electrons required to form the pair bond are contributed by the phosphorus atom which then has a residual single positive charge. As discussed earlier the bonding is probably more realistically described by the formation of 4 sp^3 hybridised σ P–O bonds and the fifth P valence electron involved in P–O π bonding with the terminal oxygens. Evidence for the scheme is the shorter P–O bond lengths compared with the calculated single bond length (see above).

Model III was devised to put a fractional charge on the bridging oxygen of -0.25. This then gave us a charge of 0.75^+ on phosphorus and -0.875 on the terminal oxygens. The Madelung potentials were calculated using the Ewald method [18].

The A and ρ parameters of the Born–Mayer function were calculated by the electron gas technique using the electron densities calculated from the wave functions determined in the appropriate Madelung potential. In Table 2 we quote mean values for each atom pair together with standard deviations. It was found that the parameters often showed a marked difference for the terminal oxygen species which has a shorter phosphorus–oxygen bond distance so a new Model IV was considered in which two

Table 3 Force constants used in the perfect lattice simulation of α-$Mg_2P_2O_7$.

Species Two-body	*Bond Length/Å*	*Force constant/eVÅ^{-2}*
$P-O_T$	1.516	35
$P-O_B$	1.590	25
Species Three-body	*Equilibrium angle/θ*	*Force constant/eVrad^{-2}*
O_TPO_T	112.33	10
O_BPO_T	106.33	15
PO_BP	144.00	20

types of O_T were used. However, this model was not proved necessary as the structure was successfully simulated using Model II.

The dispersion coefficients, C_6 terms were calculated approximately using the formulae (5) derived by Slater and Kirkwood [22]. Values for the static polarizabilities, α, and P, the effective number of electrons contributing to the polarizabilities are only known accurately for a limited number of ionic species [23]. The calculated values of C_6 which are given in Table 2, have been derived with the help of Dr Pyper [31]. Values for Mg^{2+} were taken from the literature, $\alpha = 0.486$a.u. and $P = 4.455$ [23]; for the bridging oxygen atom, O_B, we used the free atom value for the polarizability, $\alpha = 5.2$ a.u. and for the number of electrons contributing to the polarizability i.e., *s* and *p* or just *p* electrons we took the appropriate fraction of the value for neon, $P = 3.16$. For the terminal oxygen, O_T, considered to have a single negative charge the polarizability, $\alpha = 8.37$ a.u., was estimated by interpolating between our calculated value for O_B and the published value for O^{2-} in magnesium oxide [32]. The number of electrons, $P = 3.81$, was calculated by a similar method as described above for O_B. Values for P^+ polarizability were estimated on the assumption that the polarizability is roughly halved for each unit increase of nuclear charge and that this fraction increases on going down the periodic table. Values used for α and P were 17.4 a.u. and 2.54 respectively. The damping factors χ_D were estimated as follows. For the oxygen–oxygen interaction they have been set at a value of 0.5 as a mean value over a range of appropriate interionic separations [33]. Values for the phosphorus–oxygen interactions were not satisfactory and further work is required. For the magnesium–oxygen interactions the damping factor set at about 0.25 gave a reasonable simulation. The C_6 values actually used are given in Table 2.

The force constants used in the simulations are shown in Table 3. The P–O bonds were treated as harmonic oscillators.

$$E_{ij} = 1/2k(r - r_0)^2 \tag{7}$$

where $(r - r_0)$ represents the displacement from an equilibrium distance r_0(Å) and k is the spring constant. Initial values for the force constants were derived from the assigned bands in the experimental spectrum [25]. The $P-O_T$ stretching vibrations were split and occurred over a range of energies from 1052–1211 cm^{-1}. The $P-O_B$ symmetric and antisymmetric vibrations are at 740 and 982 cm^{-1} respectively. The force constants used for the three body bending terms were derived empirically starting from values which bore a sensible relation to the position of the bands in the infra red spectrum. Some adjustment was made to the force constants to give better fits to experimental structural data and from using the PHONON program with the

Table 4 Perfect crystal properties of α-$Mg_2P_2O_7$ calculated with the parameters for Model II.

Cell parameters	*Calculated*	*Experimental*
a/Å	13.29	13.20
b/Å	8.25	8.29
c/Å	8.77	8.85
β/°	104.8	104.9
Lattice Energy/eV	−311	−332 (from Born–Haber calculation)
Tensor diagonal	*Constant volume relaxation*	*Constant pressure relaxation*
Elastic constants		
$c_{11}/10^{11}$ dyn cm^{-2}	27.27	28.69
$c_{22}/10^{11}$ dyn cm^{-2}	22.09	23.84
$c_{33}/10^{11}$ dyn cm^{-2}	19.70	19.91
$c_{44}/10^{11}$ dyn cm^{-2}	7.93	8.03
$c_{55}/10^{11}$ dyn cm^{-2}	7.83	8.37
$c_{66}/10^{11}$ dyn cm^{-2}	6.29	7.27
Dielectric constants		
ε_{11}	2.43	2.33
ε_{22}	2.45	2.33
ε_{33}	3.17	3.57

wave vector q = 0.00000, 0.00000, 0.00100 to generate the frequencies and atom displacement vectors of the vibrational modes related to the infra red spectrum. The results from PHONON also test the other potential parameters as well as the force constants. The absence of imaginary eigenvalues did suggest that the simulated structure was stable and the eigenvalues calculated by the program were contained within the range of frequencies found in the experimental infra red spectrum to within 40 cm^{-1}. Because of this the locations of bands were not exactly reproduced. This indicates that our model is not yet perfect. Polarisation effects in the pyrophosphate unit could be incorporated by using the shell model and better dispersion terms may produce an improvement. Relaxation of each model of the structure to give a minimum lattice energy was attempted at constant volume and constant pressure. At constant volume the internal strains are minimised while the unit cell dimensions remain constant. The bulk strains can be and often are non-zero. At constant pressure the cell dimensions may also relax.

Our model I did not relax after a number of iterations (150) and the internal and external strains were large. In addition large negative elastic constant tensors and static dielectric constants led us to reject this model. The model with the fractional charges was also rejected as it did not improve the quality of the simulation given by Model II which by contrast relaxed within 12 iterations at constant volume and within 18 at constant pressure. The minimised lattice energies compared with values calculated from the Born Haber cycle are given in Table 4. Changes in the cell dimensions are also included in Table 4 and the diagonals of the elastic constant and static dielectric constant tensors for the constant volume and pressure relaxations are given. Although the initial fit was reasonable we investigated the effects of changing various parameters and established that by varying the A parameter for the magnesium

Table 5 Experimental (X-ray) and calculated (CONV and CONP)* bond distances and bond angles for α-$Mg_2P_2O_7$.

Species	*X-ray*	*CONV*	*CONP*
Mg (1)–O_T	2.073	2.079	2.034
	2.084	2.103	2.084
	2.135	2.087	2.133
	2.137	2.041	2.079
	2.142	2.145	2.127
	2.059	2.106	2.071
Mean value	2.105 ± 0.033	2.094 ± 0.034	2.088 ± 0.034
Mg (2)–O_T	2.037	2.024	2.011
	2.054	2.106	2.062
	2.120	2.091	2.086
	1.985	1.983	1.970
	2.024	2.131	2.098
Mean value	2.044 ± 0.044	2.067 ± 0.055	2.045 ± 0.048
P–O_B	1.612	1.558	1.583
	1.569	1.560	1.588
P–P	3.026	2.974	3.022
$< PO_BP$	144	145	145
Side I, P–O_T	1.533	1.511	1.502
	1.507	1.522	1.513
	1.472	1.507	1.496
Mean value	1.504 ± 0.025	1.513 ± 0.006	1.504 ± 0.007
$< O_TPO_T$	115	112	111
	111	111	108
	112	109	110
Side II, P–O_T	1.539	1.520	1.504
	1.527	1.526	1.519
	1.521	1.527	1.519
Mean value	1.529 ± 0.007	1.524 ± 0.003	1.514 ± 0.007
$< O_TPO_T$	115	112	109
	111	111	109
	112	107	109

*CONV and CONP denotes relaxation at constant volume and pressure respectively.

oxygen interaction from 2551.55 to 3551.55 eV and the A parameter for the phosphorus terminal oxygen from 270.72 to 300.72 eV a significantly better fit was obtained. The rationale for these changes may be that the assumption of a fully ionic model for the electron gas calculations is an over simplification. Bond distances for the atom pairs and bond angles are given in Table 5 and are compared with the experimental data. Very good agreement is obtained but detailed analysis shows that there is a tendency for the PO_3 groups in the simulated structure to become more regular than in the crystal. The angles around P tend towards the value of a regular tetrahedral angle, 109.5° and the standard deviations of the bond distances become smaller but the short phosphorus oxygen bond is reproduced in the structure relaxed at constant pressure. The P–O_B lengths become almost equal in the relaxed structure but the mean value is the same as in the crystal structure. These results, however, are not surprising when one reflects that the electron gas and other parameters were averaged. The magnesium–oxygen bond lengths at both magnesium sites are well produced. The sixfold coordination at the first site and the fivefold coordination at the second site is simulated correctly and the short Mg–O bond of 1.98 Å at the second site is also reproduced correctly.

5 CONCLUSIONS

The work described has demonstrated that molecules of the complexity of pyrophosphates can be simulated successfully. Good agreement between the calculated and experimental structures of α-magnesium pyrophosphate has been obtained and the lattice energy compared well with that calculated from the Born-Haber thermochemical cycle.* The pyrophospate anion modelled best using formal rather than fully ionic charges. There was a slight tendency for the phosphate units to model as regular terahedra. The model could be refined to take account of this tendency. Nevertheless we feel confident that the model can form the basis of our investigations into the substitution defects of cations in many biominerals.

Acknowledgements

The authors would like to thank Dr A.H. Harker, AEA Technology, Harwell for calculating the wave functions for the derivation of the interatomic potentials using the electron gas method and for helpful discussions with Dr R.G.J. Ball; Dr. N.C. Pyper, University of Cambridge for his help in the calculations of the dispersion coefficients. The simulations were performed on the University of Reading's AMDAHL 5870 and a SUN SPARC station 1. Dr M.G. Taylor is grateful for funding from the University of Reading's Endowment Fund and the Leverhulme Trust.

APPENDIX: ESTIMATION OF THE EXPERIMENTAL LATTICE ENERGY FOR α-MAGNESIUM PYROPHOSPHATE

The lattice energy, Equation (1), is estimated from thermochemical data outlined below. Numerical values are $\Delta H_{298}/kJ\,mol^{-1}$.†

$$2Mg^{2+}_{(g)} + P_2O^{4-}_{7(g)} \rightarrow Mg_2P_2O_{7(c)} \qquad (1)$$

(a) Heat of formation of Mg^{2+}: 2326

$$Mg_{(c)} \rightarrow Mg_{(g)} \rightarrow Mg^{2+}_{(g)}$$

(b) Heat of formation of the $P_2O_7^{4-}$ ion: 6524

$$(HO)_2OPOPO(OH)_{2(l)} \rightarrow P_2O_{7(g)} + 4H_{(g)} \rightarrow P_2O^{4-}_{7(g)} + 4H^{+}_{(g)}$$

(taking the electron affinity for $O_{(g)} \rightarrow O^{-}_{(g)}$)

(c) Heat of formation of magnesium pyrophosphate crystal: −2901

$$2MgO_{(c)} + H_4P_2O_{7(l)} \rightarrow Mg_2P_2O_{7(c)} + 2H_2O_{(l)}$$

(d) Lattice energy of magnesium pyrophosphate: −8275

$$[(a) + (b) + (c) + (d) = 0 \text{ (Born Haber)}]$$

*See Appendix for details of the calculation.

†$1\,eV \approx 97\,kJ\,mol^{-1}$.

References

[1] J. Christoffersen and W.J. Landis, "A contribution with Review to the Description of Mineralization of Bone and Other Calcified Tissues *in Vivo*", *The Anatomical Record*, **230,** 435 (1991).

[2] R.G.G. Russell, A.M. Caswell, P.R. Hearn and R.M. Sharrard, "Calcium in mineralized tissues and Pathological Calcification", *Brit. Med. Bull.*, **42,** 435 (1986).

[3] K. Simkiss, M.G. Taylor and G.N. Greaves, "Form of the Anion in the Intracellular Granules of the Crab", *J. Inorganic Biochem.*, **39,** 17 (1990).

[4] M.G. Taylor and K. Simkiss, "Structural and Analytical Studies on Metal Ion-Containing Granules", In *Biomineralization*, eds. S. Mann, J. Webb and R.J.P. Williams, VCH Weinham, (1989), ch 13.

[5] G.M. Clark and R. Morley, "Inorganic Pyro-compounds $M_a[(X_2O_7)_b]$", *Chem. Soc. Revs*, **5,** 269 (1976).

[6] N.C. Webb, "The Crystal Structure of β-$Ca_2P_2O_7$", *Acta Cryst.*, **21,** 942 (1966).

[7] C. Calvo, "The Crystal Structure of α-$Ca_2P_2O_7$', *Inorg. Chem.*, **7,** 1345 (1968).

[8] C. Calvo, "Refinement of the Crystal Structure of β-$Mg_2P_2O_7$", *Can. J. Chem.*, **43,** 1139 (1965).

[9] M. O'Keeffe, B. Domengès and G.V. Gibbs, "*Ab initio* Molecular Orbital Calculations on Phosphates: Comparison with Silicates", *J. Phys. Chem.*, **89,** 2304 (1985).

[10] D.W.J. Cruickshank, "The Role of 3*d*-orbitals in π-Bonds between (a) Silicon, Phosphorus, Sulphur or Chlorine and (b) Oxygen or Nitrogen", *J. Chem. Soc.*, 5486 (1961).

[11] N.S. Mandel, "The Crystal Structure of Calcium Pyrophosphate Dihydrate", *Acta Cryst.*, **B31,** 1730 (1975).

[12] L. Pauling, in "The Nature of the Chemical Bond", Oxford University Press, 3rd ed., (1960).

[13] Y. Abe and H. Hosono, "Phosphate Glasses and Glass-Ceramics", in *Inorganic Phosphate Materials*, ed T. Kanazawa, Elsevier 1989, ch 10.

[14] C. Calvo, "The Crystal Structure of α-$Mg_2P_2O_7$", *Acta Crystal.*, **23,** 289 (1967).

[15] P.R. Adby and M.A.H. Dempster, in "*Introduction to Optimization Methods*", Chapman and Hall, (1974).

[16] C.R.A. Catlow, C.M. Freeman and R.L. Royle, "Recent Studies using static simulation techniques", *Physica*, **131B,** 1 (1985).

[17] R.A. Jackson and C.R.A. Catlow, "Computer Simulation Studies of Zeolite Structure", *Molec. Simul.*, **207,** 1, (1988).

[18] M.P. Tosi, "Cohesion of Ionic Solids in the Born Model", *Solid State Phys.*, **16,** 1 (1964).

[19] M. Leslie, "A three-body potential model for the static simulation of defects in ionic crystals", *Physica B*, **131,** 145 (1985).

[20] A.J.M. de Man, B.W.H. van Beest, M. Leslie and R.A. van Santen, "Lattice Dynamics of Zeolitic Silica Polymorphs", *J. Phys. Chem.*, **94,** 2524 (1990).

[21] C.R.A. Catlow and A.M. Stoneham, "Ionicity in solids", *J. Phys. C*, **16,** 4321 (1983).

[22] J.C. Slater and J.G. Kirkwood, "The Van der Waals Forces in Gases", *Phys. Rev.*, **37,** 682 (1931).

[23] N.C. Pyper, "Relativistic *ab initio* Calculations of the Properties of Ionic Solids", *Phil., Trans. R. Soc. Lond.*, **A320,** 107, (1986).

[24] M.G. Taylor, unpublished work.

[25] A.N. Lazarev, in "Vibrational Spectra and Structure of Silicates", Consultants Bureau: New York, (1972).

[26] J.H. Harding and A.H. Harker, "The Calculations of Interatomic Potentials using Electron-Gas Models", *UKAEA Harwell Report*, AERE R10425, (1982).

[27] P.T. Wedepohl, "Influence of electron distribution on atomic interaction potentials", *Proc. Phys. Soc.*, **92,** 79 (1967).

[28] R.G. Gordon and Y.S. Kim, "Theory for the Forces between Closed-Shell Atoms and Molecules", *J. Chem. Phys.*, **56,** 3122 (1972).

[29] B.G. Dick, Jr. and A.W. Overhauser", Theory of the Dielectric Constants of Alkali Halide Crystals", *Phys. Rev.*, **112,** 90 (1958).

[30] R.A. Jackson, "Computer Simulation of Inorganic Materials" in "*Computer Modelling of Fluids, Polymers and Solids*" eds. C.R.A. Catlow, S.C. Parker and M.P. Allen. *NATO ASI Series C*, 293 ch 15 (1990).

[31] N.C. Pyper, personal communication, (1991).

[32] P.W. Fowler, P.J. Knowles and N.C. Pyper, "Calculations of two-and three-body dispersion coefficients for ions in crystals", *Molec. Phys.*, **56,** 83 (1985).

[33] R.G.J. Ball and P.G. Dickens, "Calculation of Structural and Defect Properties of α-U_3O_8", *J. Mater. Chem.*, **1,** 105 (1991).

[34] T.L. Woods and R.M. Garrels, "Thermodynamic values for natural and inorganic materials", OUP (1987).

[35] H.E. Barner and R.V. Scheuerman, "Handbook of thermochemical data", Wiley Interscience (1978).

[36] J.G. Stark and H.G. Wallace, "Chemistry Data Book" John Murray, (1976).